Thermochimica Acta, 130 (1988) 309–318
Elsevier Science Publishers B.V., Amsterdam – Printed in The Netherlands

HIGH TEMPERATURE X-RAY DIFFRACTION TECHNIQUES FOR ENHANCING TIME/TEMPERATURE RESOLUTION

PHILIP ENGLER, MARK W. SANTANA, MARTIN L. MITTLEMAN and DAVID BALAZS

BP America Research and Development, 4440 Warrensville Center Road, Cleveland, OH 44128 (U.S.A.)

(Received 17 November 1987)

ABSTRACT

In situ, high temperature X-ray diffraction offers an advantage over traditional thermal analysis techniques (e.g. DSC, DTA and TG) in that only XRD allows identification of specific reactants and reaction products. Recent improvements in X-ray sources and detectors now allow higher time and temperature resolution between individual diffractograms. As a result it is now possible to acquire diffractograms corresponding to narrow temperature ranges while continuously heating a sample. For example, with the high intensity of a rotating anode X-ray generator, a temperature resolution of 4 °C was obtained while heating dolomite at 3 °C min^{-1} to elucidate its decomposition mechanisms. When the higher flux was combined with a position sensitive detector, a time resolution of 12 s, which corresponded to a temperature resolution of 0.86 °C, was obtained upon heating potassium sulfate at 4 °C min^{-1}. The data from these scans allowed the extent of reaction for specific phases to be plotted as a function of temperature. These plots showed excellent agreement with similar data obtained by DSC and TG analyses.

INTRODUCTION

Conventional thermal analysis techniques, e.g. differential scanning calorimetry and thermogravimetric analysis, allow determination of the energy required for a reaction and the weight change of a sample during a reaction as a function of temperature, time and heating rate. However, thermal analysis techniques alone cannot identify the reaction products that result from each thermal event, and thus cannot fully characterize the reaction. Identification of these products requires analytical techniques such as X-ray diffraction (XRD), infrared and Raman spectroscopy, mass spectrometry and gas chromatography. Of these techniques, XRD is often the most appropriate for characterizing reactions when crystalline materials are involved as either reactants or products.

While samples can be removed from a thermal analysis instrument at progressive stages of thermal treatment for XRD characterization, in situ,

0040-6031/88/$03.50 © 1988 Elsevier Science Publishers B.V.

high temperature XRD offers several advantages over this mode. First, in situ analyses eliminate the need for multiple samples. Second, in situ experiments allow observation of metastable, high temperature phases that might otherwise be lost upon cooling. Since intermediate structures can be elucidated, in situ analyses allow the kinetics of a reaction or transformation to be followed. Also, in situ experiments prevent the anomalies that may occur when a series of specimens are not placed precisely back into the same position of the instrument sample chamber after heat treating.

Recent examples of in situ XRD include investigations of the decomposition of carbonate minerals [1,2], limestone sulfation [2], thermally induced reactions in phosphate conversion coating for steel [3] and the temperature dependence of unit cell parameters of polymers [4]. These studies, which were performed with sealed tube X-ray sources and scintillation detectors, required 5–25 min for each scan when multiple peaks were analyzed. "Ramp and hold" rather than continuous heating schedules were used for non-isothermal investigations because X-ray diffractograms obtained under the latter conditions would have covered too broad a temperature range.

Obtaining X-ray data while continuously heating a sample requires that data acquisition time be reduced so that each scan corresponds to a narrow temperature interval. One way of accomplishing this is to use a more efficient detector. For example, Fawcett et al. [5] used a position sensitive detector (PSD), which allows simultaneous data collection over a wide 2θ range, to study the behavior of pharmaceuticals at 5 °C intervals while heating samples at 1 °C min^{-1}. Similarly, Crowder et al. [6] investigated the melting and crystallization behavior of polyethylene by collecting X-ray data at 2 °C intervals. Alternatively or concurrently, data acquisition time can be reduced by increasing the X-ray flux. Russell and Koberstein [7] used a synchrotron source to obtain scans with an interval of less than 1 °C while heating and cooling polyethylene. Their heating rate was 10 °C min^{-1} and their scan time was 5 s.

Rotating anode generators provide another way for increasing intensity. Although the flux from a rotating anode is not nearly as intense as from a synchrotron source, it still offers a significant increase in intensity compared to conventional sealed tube sources. For example, the intensity from a copper rotating anode source operated at 50 kV and 200 mA is approximately ten times greater than from a sealed copper anode tube operated at 40 kV and 30 mA. This translates to an order of magnitude reduction in data acquisition time without any degradation of the signal. In addition, a rotating anode generator in one's own laboratory offers the important advantage of accessibility.

This paper demonstrates the excellent temperature resolution that can be obtained for continuous heating programmed, in situ XRD by reducing data acquisition time to 10–30 s. This was accomplished by using a rotating anode generator either with a PSD or a scintillation detector.

EXPERIMENTAL

All XRD measurements were made with a Rigaku X-ray diffraction system consisting of a 1400 °C attachment mounted on a horizontal, wide angle goniometer interfaced with a 12 kW rotating anode, X-ray generator. The generator was operated at 50 kV and 200 mA. Cu K_α radiation was used for all experiments. For measurements with a scintillation detector, monochromatic radiation was obtained through the use of a curved, graphite crystal monochromator between the sample and the detector. Measurements with a position sensitive detector were made by replacing the scintillation detector, receiving slit and monochromator with a Braun 5 cm, straight PSD interfaced to a Braun 64K channel, multichannel analyzer (MCA) and a nickel filter. This detector contains a 50 mm long, carbon coated, quartz wire with 0.05 mm resolution. When set at a distance of 185 mm from the sample, this PSD covers an angular range of approximately 13° 2θ with a maximum resolution of 0.013° 2θ per channel.

Approximately 500 mg of sample, which had been hand ground in an agate mortar and pestle to pass through 325 mesh ($< 44\ \mu$m), were packed in the platinum holder of the high temperature attachment. After closing the attachment, the sample chamber was either purged with air (700–800 ml min^{-1}) or CO_2 (550–650 ml min^{-1}), with the purge being continued for the duration of the experiment.

For measurements with the scintillation counter, the sample was heated at a nominal rate of 3 °C min^{-1}; however, the rate varied between 1.5 °C and 4.5 °C min^{-1} ($\sigma = 0.8$° C min^{-1}). The sample was scanned at 40° 2θ min^{-1} from 25° to 45° 2θ with approximately 50 s between each scan. These conditions provided a temperature resolution between scans of 2–6 °C with each 30-s scan covering 0.75–2.25 °C. For measurements with the PSD, the nominal heating rate was 4.3 °C min^{-1} with a range characterized by a standard deviation of 0.7 °C min^{-1}. The multichannel analyzer was set to collect data for 10 s with 2-s intervals between data sets. These conditions provided a nominal temperature resolution of 0.86 °C ($\sigma = 0.14$ °C) with each scan covering 0.72 °C ($\sigma = 0.12$ °C).

Differential scanning calorimeter (DSC) scans were obtained at 3 °C min^{-1} under 50 ml min^{-1} of nitrogen using the DuPont 910 DSC module. Sample size was 10–20 mg. Thermogravimetric (TG) analysis scans were obtained at 3 °C min^{-1} under 50 ml min^{-1} of CO_2 using the DuPont 951 TGA module. Sample size was approximately 95 mg. Both modules were interfaced to a DuPont 1090 data analysis system.

Sample thermocouples for the high temperature XRD stage and DSC were calibrated by using potassium nitrate and potassium sulfate, which undergo solid state crystalline phase transformations at 128 and 583 °C, respectively [8]. Table 1 shows excellent agreement between transition temperatures obtained from the high temperature stage, differential scanning

TABLE 1

Temperature calibration of high temperature XRD attachment and DSC (transition temperatures (°C))

(a) KNO_3

	XRD PSD	XRD Scint Run 1	XRD Scint Run 2	DSC	ICTA Standard [a]
Start	129	121–127	128–130	127	
Extrapolated onset				129.4	128 ± 5
Peak				131.8	135 ± 6
Finish	132–134	127–131	132–142	141	

(b) K_2SO_4

	XRD PSD	XRD Scint	DSC	ICTA Standard [a]
Start	569–570	573–577	567	
Extrapolated onset			579.9	582 ± 7
Peak			581.7	588 ± 6
Finish	586–587	585–591	586	

[a] Ref. 9.

calorimetry and the literature [9]. The start temperature range for XRD was defined by the temperature for the scan at which the phase transformation could first be detected and the temperature of the previous scan. Similarly, the finish temperature range was defined by the last scan at which the low temperature phase could be detected and the next scan. The range limits for the scans using the PSD were more precise than those with the scintillation detector due to the higher temperature resolution of the former. Start and finish temperatures for the DSC scans were the temperatures at which the signal first departed from and finally returned to the baseline, respectively. Extrapolated onset temperature was defined as the intersection of the forward-extrapolated, low temperature side baseline with the back-extrapolated, initial side of the peak. DSC peak temperature was taken at the peak minimum.

The materials used in this study included potassium nitrate (Baker analyzed reagent grade), potassium sulfate (Fisher certified grade), and dolomite (Wards, determined by ICP-AES to be $Ca_{1.00}$ $(Mg_{0.99}Fe_{0.01})(CO_3)_2$ with 0.4% SiO_2).

RESULTS AND DISCUSSION

Rotating anode / scintillation detector

In order to demonstrate how increased incident intensity can improve the information available from X-ray diffraction, dolomite was decomposed in

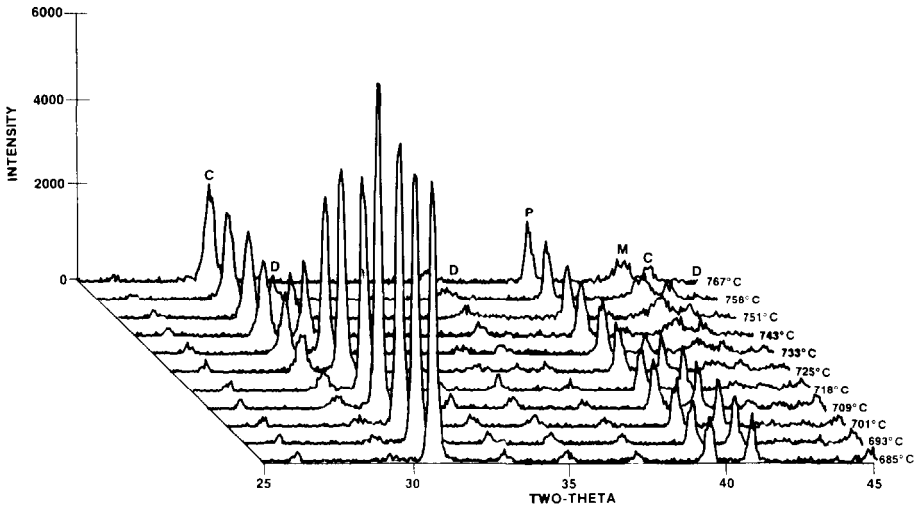

Fig. 1. XRD patterns of dolomite heated in situ at 3°C min^{-1} under a CO_2 atmosphere showing the first stage of decomposition. Patterns were obtained by scanning at 40° 2θ min^{-1} with a scintillation detector (C = $CaCO_3$, D = dolomite, M = MgO, P = platinum sample holder).

the high temperature attachment under CO_2 using a conventional scintillation detector with the X-ray generator set at 50 kV and 200 mA. It is generally agreed that formation of $CaCO_3$ corresponds to the first step of dolomite decomposition under CO_2, but controversy exists over the actual reaction occurring during the first stage. Two proposed reactions include direct formation of $CaCO_3$ accompanied by the formation of either MgO or of $MgCO_3$. In the latter case, the $MgCO_3$ would further decompose to MgO. Alternatively, the first reaction has been attributed to primary dissociation into oxides followed by recarbonization to $CaCO_3$ [10]. In situ X-ray scans of dolomite as it decomposed provided answers to these alternatives.

Figure 1, which displays every second scan acquired, summarizes the 21 scans that were acquired between 685 and 767°C at 4°C intervals. These data show that dolomite under CO_2 decomposed directly to $CaCO_3$ accompanied by the formation of MgO. No evidence was offered for the formation of either CaO or $MgCO_3$. This supports the reaction

$$CaMg(CO_3)_2 \rightarrow CaCO_3 + MgO + CO_2 \quad (1)$$

as being responsible for the first stage of dolomite decomposition under a CO_2 atmosphere. Furthermore, the growth of the peak at 29.2° 2θ rather than a gradual shifting of the dolomite peak from 30.6° 2θ suggested the formation of discrete $CaCO_3$ rather than a gradual change in the composition of the solid solution toward the end member. The phases formed by the first reaction were stable to 914°C where the second step of the reaction

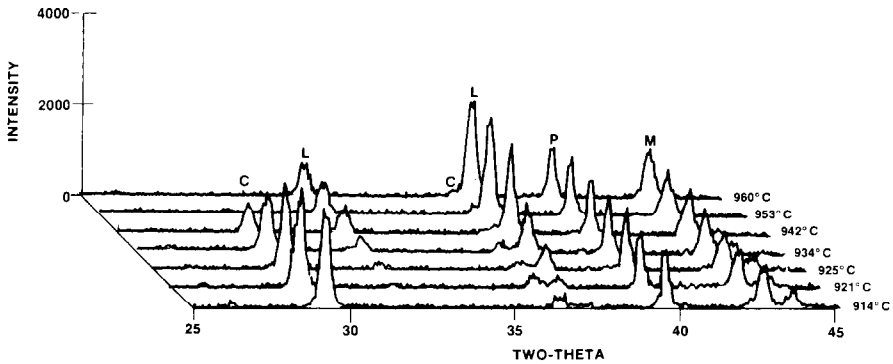

Fig. 2. XRD patterns of dolomite decomposition products heated in situ at 3 °C min^{-1} under a CO_2 atmosphere showing the second stage of decomposition. Patterns were obtained by scanning at 40° 2θ min^{-1} with a scintillation detector (C = $CaCO_3$, L = CaO, M = MgO, P = platinum sample holder).

began. Figure 2 (showing every second scan) reveals that the reaction expressed by

$$CaCO_3 \rightarrow CaO + CO_2 \tag{2}$$

was complete by 960 °.

The gain obtained by using the rotating anode really stands out when obtaining quantitative and kinetics information about a reaction. The relative content of any phase as a function of temperature can be calculated by normalizing the X-ray peak areas for that phase to the maximum area obtained for that phase. Figure 3 shows the temperature dependence of peak area for dolomite ($2\theta = 30.6°$), $CaCO_3$ (29.2°) and CaO (32.0°) in CO_2. For these figures, data were obtained from each scan so that each point represents a 1.5 °C interval taken every 4 °C. Peak areas were normalized to the average area existing after the completion of a reaction for a product and before the start of a reaction for a reactant. These plots are equivalent to the extent of reaction α for a phase decomposing and $(1 - \alpha)$ for a phase being formed. Although beyond the scope of this paper, the data expressed in the form of α or $(1 - \alpha)$ versus temperature can be used to obtain kinetic parameters, e.g., apparent activation energy and reaction order, using the various models in the literature for non-isothermal experiments.

The extent of reaction at any temperature, T, can also be calculated from TG data using the following equation

$$\alpha = \frac{\text{(Initial sample weight)} - \text{(Sample weight at } T\text{)}}{\text{Weight loss for step}} \tag{4}$$

Figure 4 compares the XRD and TG data. The excellent agreement between the results obtained by the two analytical methods shows the validity of using X-ray data to characterize the kinetics of a reaction.

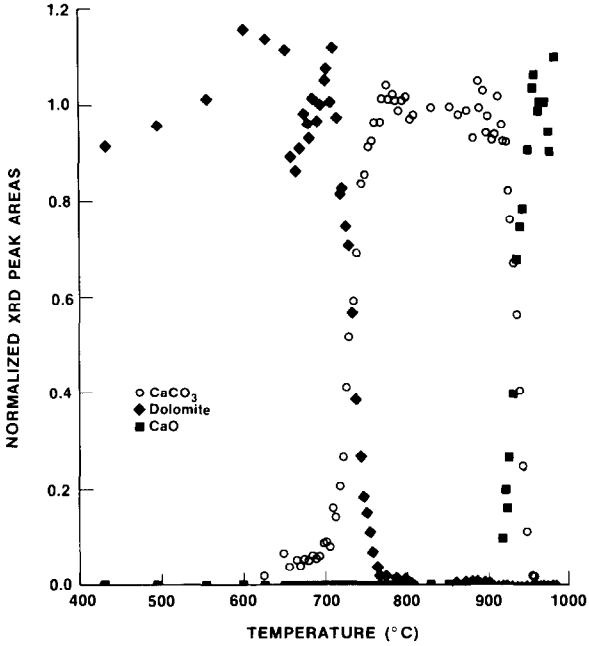

Fig. 3. Normalized XRD peak areas for dolomite and its decomposition products under CO_2 ($CaCO_3$, 29.2° 2θ; dolomite, 30.6° 2θ; CaO, 32.0° 2θ).

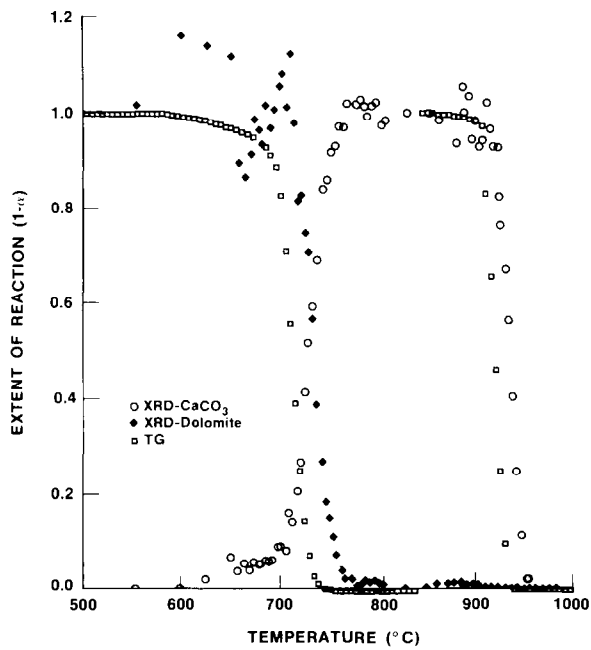

Fig. 4. Comparison of extent of reaction $(1-\alpha)$ under CO_2 of dolomite and its decomposition products obtained by XRD and by TG.

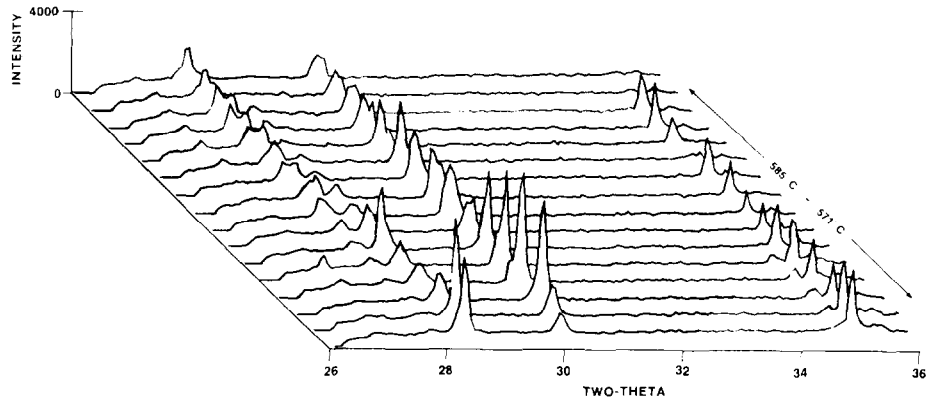

Fig. 5. XRD patterns of K_2SO_4 heated in situ at 4 °C min^{-1} showing phase transformation. Patterns were obtained by collecting data with a PSD for 10 s with 2 s between patterns.

Rotating anode / position sensitive detector

As an example of the time/temperature resolved data that can be obtained by combining a PSD with a rotating anode generator, Fig. 5 shows sixteen consecutive diffractograms spanning 15 °C that were obtained for potassium sulfate while this material underwent a phase transition. The entire reaction required 23 diffractograms spanning 18 °C. In contrast, only seven diffractograms could be obtained for this reaction using the scintillation detector in a scanning mode (Fig. 6, which shows only 10 of the 20 ° 2θ that were scanned).

The true value of the PSD may come not in the increase in signal to noise ratio but in its ability to record the data simultaneously over a range of angles. Recall that for the scintillation detector scans, 80 s (corresponding to 4 °C) elapsed between times that the detector arm was at a specific 2θ position. Transient peaks such as the one detected with the PSD at 32 °C 2θ in Fig. 7 would have been missed with a scintillation detector unless the detector had been in the correct 2θ position while the peak was present.

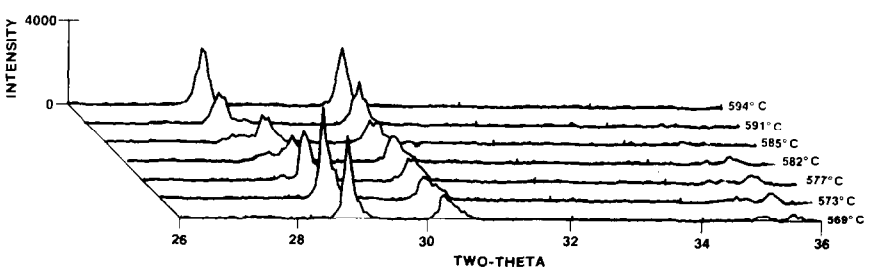

Fig. 6. XRD patterns of K_2SO_4 heated in situ at 4 °C min^{-1} showing phase transformation. Patterns were obtained by scanning at 40 ° 2θ min^{-1} with a scintillation counter with 80 s between the start of each scan.

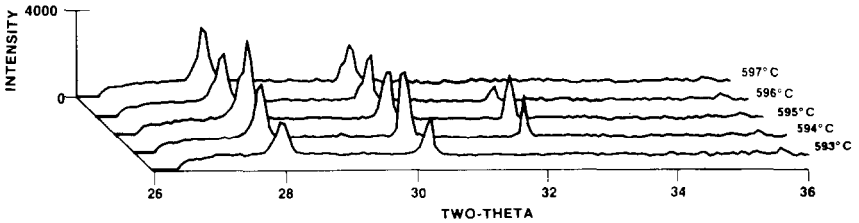

Fig. 7. XRD patterns of K_2SO_4 heated in situ at 4°C min^{-1} showing transient behavior. Patterns were obtained by collecting data with a PSD for 10 s with 2 s between patterns.

As with dolomite, the temperature dependence of peak areas corresponding to the low ($2\theta = 28.0°$) and high ($2\theta = 28.5°$) temperature phases of K_2SO_4 relates directly to the extent of the transformation (Fig. 8). Figure 8 also shows the extent of reaction for the K_2SO_4 reaction calculated from DSC data. The last data were obtained by measuring the partial peak area of the transformation endotherm, ΔH_t, normalized by the total area, ΔH_f, as a function of temperature

$$\alpha = \Delta H_t / \Delta H_f \tag{5}$$

Figure 8 shows the good agreement between the temperature dependence of the transformation as measured from XRD peak areas and as measured by DSC, which uses more accurate and precise heating stages. The 4–5° offset

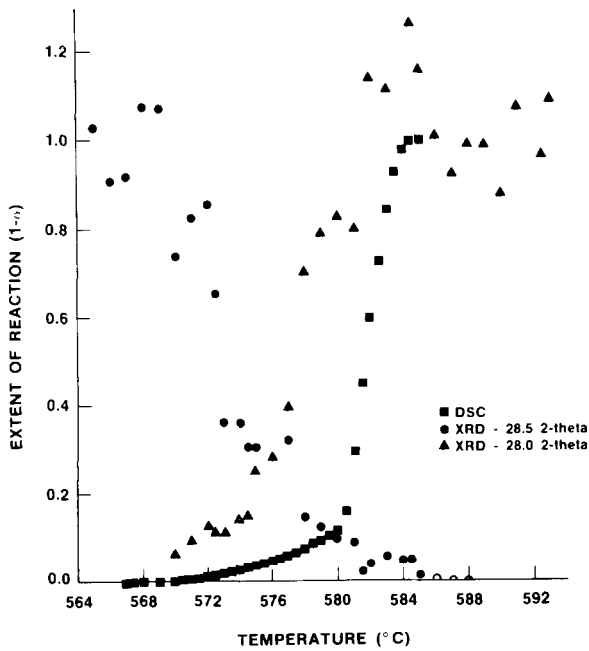

Fig. 8. Comparison of extent of reaction $(1 - \alpha)$ for phase change of K_2SO_4 obtained by XRD and by DSC.

between the XRD and DSC data is reasonable considering the degree of scatter in the X-ray data.

CONCLUSIONS

Improvements in SNR allow time and temperature resolved, in situ, high temperature X-ray data to be obtained. For example, with a rotating anode alone, a temperature resolution of 4 °C was obtained while heating dolomite at 3 °C min^{-1}. When combined with the PSD, a temperature resolution of 0.86 °C, corresponding to one 13° 2θ pattern every 12 s, was obtained upon heating potassium sulfate at 4 °C min^{-1}. These data allowed the extent of reaction for a specific phase to be plotted as a function of temperature. These plots agreed quite well with similar data obtained by thermal analysis (DSC and TG). However, the X-ray technique offers an advantage over thermal analysis techniques in that only the former allows changes in specific reactants and reaction products to be resolved.

ACKNOWLEDGMENTS

We wish to thank Peter Calendra and Kenneth O'Brien of Innovative Technology, Inc. (So. Hamilton, MA) for loaning us the Braun PSD that was used in this study.

REFERENCES

1 S.S. Iyengar, P. Engler, M.W. Santana and E.R. Wong, in C.S. Barrett, P.K. Predecki and D.E. Leyden (Eds.), Advances in X-ray Analysis, Vol. 28, Plenum Press, New York, 1985, p. 331.
2 D.E. Anderson and W.J. Thomson, Ind. Eng. Chem. Res., 26 (1987) 1628.
3 R. Bartoszek-Loza and R.J. Butler, Poly. Mater. Sci. Eng., 55 (1986) 557.
4 G.A. Jones and H.W. Starkweather, J. Macromol. Sci. Phys., B24, (1985–1986) 131.
5 T.G. Fawcett, E.J. Martin, C.E. Crowder, P.J. Kincaid, A.J. Strandjor, J.A. Blazy, D.N. Armentrout and R.A. Newman, in C.S. Barrett, J.B. Cohen, J. Faber, R. Jenkins, D.E. Leyden, J.C. Russ and P.K. Predecki (Eds.), Advances in X-ray Analysis, Vol. 29, Plenum Press, New York, 1986, p. 323.
6 C.E. Crowder, S. Wood, B.G. Landes, R.A. Newman, J.A. Blazy and R.A. Bubeck, in C.S. Barrett et al. (Eds.), Advances in X-ray Analysis, Vol. 29, Plenum Press, New York, 1986, p. 315.
7 T.P. Russell and J.T. Koberstein, J. Polym. Sci. Polym. Phys. Ed., 23 (1985) 1109.
8 NBS Circular 500, Selective Values of Chemical Thermodynamic Properties, 1952.
9 Certificate—ICTA Certified Reference Materials for Differential Thermal Analysis, Differential Scanning Calorimetry and Related Techniques from 125–940 °C. Certified by the International Confederation for Thermal Analysis and Distributed by the United States National Bureau of Standards as GM-758, GM-759 and GM 760.
10 R. Otsuka, Thermochim. Acta, 100 (1968) 69.